NACA RM E56K29b

NACA

RESEARCH MEMORANDUM

INTERNAL PERFORMANCE OF TWO-DIMENSIONAL WEDGE EXHAUST NOZZLES

By William T. Beale and John H. Povolny

Lewis Flight Propulsion Laboratory
Cleveland, Ohio

NATIONAL ADVISORY COMMITTEE FOR AERONAUTICS

WASHINGTON

February 28, 1957
Declassified December 3, 1958

NATIONAL ADVISORY COMMITTEE FOR AERONAUTICS

RESEARCH MEMORANDUM

INTERNAL PERFORMANCE OF TWO-DIMENSIONAL WEDGE EXHAUST NOZZLES

By William T. Beale and John H. Povolny

SUMMARY

An experimental investigation of four rectangular-throat two-dimensional wedge exhaust nozzles was conducted. Three of the nozzles were designed to conform to Prandtl-Meyer streamlines for pressure ratios of 5, 10, and 24; and a fourth, arbitrarily contoured, with a length less than that required for isentropic expansion, was designed for a pressure ratio of about 9. The effects of variations in the side plate, the lip angle, and the geometry upstream of the throat were investigated on the nozzle designed for a pressure ratio of 10.

The three Prandtl-Meyer wedge nozzles tested were determined to have peak thrust coefficients about 1 percent lower than those of the best convergent-divergent and plug nozzles investigated to date; the thrust at all pressure ratios below design was within about $3\frac{1}{2}$ percentage points of the peak thrust. The variations in approach-section size and lip angle had negligible effect on thrust over the ranges tested, and a 50-percent reduction in side-plate coverage caused about a 1-percentage-point thrust-coefficient loss. The shortened wedge showed a peak thrust coefficient about 2 percent below those of the best Prandtl-Meyer designs tested.

INTRODUCTION

As flight speeds increase, the aircraft exhaust nozzle becomes increasingly important; slight gains in nozzle thrust coefficient, or reductions in its drag, weight, or cooling load, are reflected in significant improvements in over-all aircraft performance. In order to attain such improvements, the NACA Lewis laboratory has extended its exhaust-nozzle research program to include an experimental investigation of the wedge nozzle, a type which, it is believed, may have installation advantages in some applications (twin-pod or underbody installations, e.g.) over the previously considered convergent-divergent nozzles, divergent ejectors, and plug nozzles (refs. 1 to 3).

The wedge nozzles investigated are defined as those utilizing two-dimensional expansion from a corner and having a free-jet boundary

downstream of this corner. They are similar in principle to the "pen-shape" exit reported in reference 4 except for the fact that they use a two-dimensional wedge for the expansion surface. Their geometry and nomenclature are described in the following sketch:

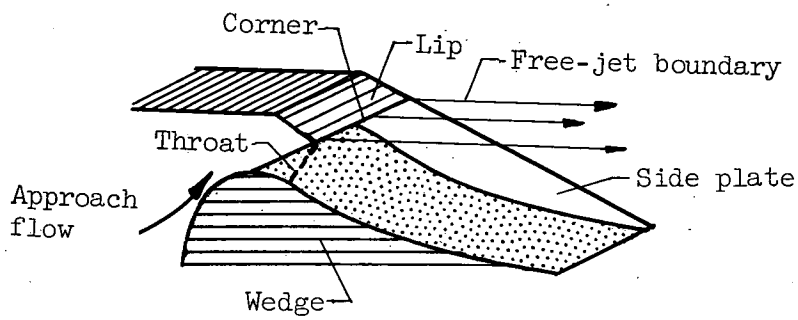

These nozzles may be designed to conform to streamlines in Prandtl-Meyer flow and hence can provide essentially isentropic expansion at their design pressure ratio. Furthermore, the presence of the free-jet boundary allows the expanding jet to be influenced by ambient pressure changes as it is with the external expansion plug. The wedge nozzle may then be expected to exhibit moderate variations in thrust coefficient with pressure ratio as does the plug nozzle, thereby reducing the necessity of geometrical variations with flight Mach number.

This report gives results of an experimental investigation of three rectangular-throat wedge nozzles designed to conform to Prandtl-Meyer streamlines for pressure ratios of 5, 10, and 24. Variations in the side plate, the lip angle, and the geometry upstream of the throat were made on the nozzle designed for a pressure ratio of 10. A fourth wedge with length less than that required for isentropic expansion was also tested. The effect of these geometry changes and some general characteristics of wedge nozzles are discussed.

APPARATUS AND INSTRUMENTATION

Wedge-Nozzle Configurations

The three wedge contours used with the Prandtl-Meyer wedge nozzles (described in fig. 1) conform to streamlines resulting from the expansion of a compressible fluid (air) around a sharp corner (Prandtl-Meyer flow). These contours are based on the tabular information given in reference 5, in which the assumption of a straight sonic line at the throat of the nozzle is made. No boundary-layer correction was included. An arbitrarily contoured wedge shorter than the Prandtl-Meyer designs is shown in figure 2. Tabulations of the coordinates of the wedge surfaces are presented on both figures 1 and 2.

The general construction features common to the wedge configurations tested are illustrated in figure 3. All configurations were of the double-wedge type with cantilevered lips bolted as shown.

Test Facility

A schematic drawing of the test facility is given in figure 4. The nozzles were mounted on a pipe freely suspended by flexure rods which were connected to the bedplate. Pressure forces acting on the nozzle and mounting pipe were transmitted from the bedplate through a flexure-plate-supported bell crank and linkage to a balanced-air-pressure-diaphragm force-measuring cell. Pressure differences across the nozzle and mounting pipe were maintained by labyrinth seals around the mounting pipe, which separated the nozzle-inlet air from the exhaust. The space between the two labyrinth seals was vented to the test chamber. This decreased the pressure differential across the second labyrinth and prevented a pressure gradient on the outside of the diffuser section which could result from airflow through the labyrinth seal.

Instrumentation

Pressures and temperatures were measured at the various stations indicated in figure 4. One wall static- and six total-pressure measurements at station 1 were used to compute inlet momentum, and eight total- and two wall static-pressure measurements at station 2 were used to compute airflow. Eight total-pressure and one temperature measurements were made at the nozzle inlet (station 3). Ambient exhaust-pressure measurement was provided at station 0, and a static-pressure survey was made on the outside walls of the bellmouth inlet. Wall static pressures were measured along the wedge surfaces from throat to tip.

PROCEDURE

Performance data for each configuration were obtained over a range of nozzle pressure ratios at a constant airflow. The nozzle pressure ratio was varied from about 2 to the maximum obtainable (26 to 32). For all tests the nozzle total pressure was within the range of 50 to 60 inches of mercury absolute.

The thrust coefficient was calculated by dividing the actual jet thrust by the ideal jet thrust. The actual jet thrust was computed by subtracting the force measured by the balanced-air-pressure diaphragm from the inlet total momentum as measured by pressure and temperature instrumentation at station 1 and corrected for bellmouth and labyrinth forces. The ideal jet thrust is defined as the product of the measured

mass flow and the ideal jet velocity (assuming isentropic expansion) based on the measured nozzle pressure ratio and inlet temperature.

The symbols used in this report are defined in appendix A, and the equations used in the calculations are given in appendix B.

Standard 25° half-angle convergent nozzles were used at the beginning and end of the test program. The results (fig. 5) show the order of repeatability of thrust and flow coefficients to be within 0.5 percent. Similar tests, with similar results, were made during the nozzle programs reported in references 1 to 3. The thrust data contained in these and the present report are thus directly comparable.

The maximum possible error in thrust data in this report was estimated from possible experimental errors in reading the primary quantities used to compute thrust: total and static pressures, areas, forces, tares, and the like. A value of ±1.5 percent was obtained.

RESULTS AND DISCUSSION

General Wedge-Nozzle Characteristics

Some features common to all the wedge-nozzle data (figs. 6 to 11) are described in the following sketches and discussion. As shown in the

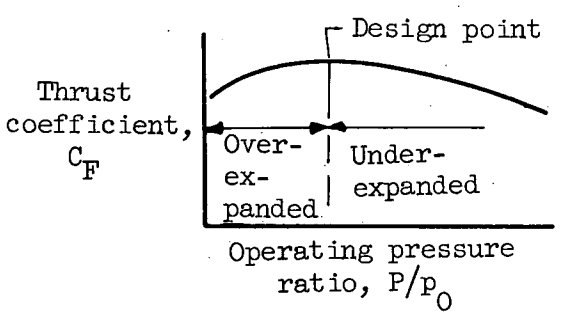

preceding sketch, the peak thrust coefficient occurs at or near the design pressure ratio, which is defined as the pressure ratio required to permit one-dimensional isentropic expansion from uniform sonic flow at the geometrical throat area to uniform supersonic flow through the exit area. At such a pressure ratio the flow should be discharged uniformly in the axial direction at the ambient static pressure. Ideally, no losses should occur under these conditions; but the actual thrust is, of course, affected by wall friction, improper wedge shape, and departure from the assumed sonic line at the throat, all contributing to thrust loss.

As shown in the next sketch, at pressure ratios less than design (the overexpanded region), the flow expands part way down the wedge to

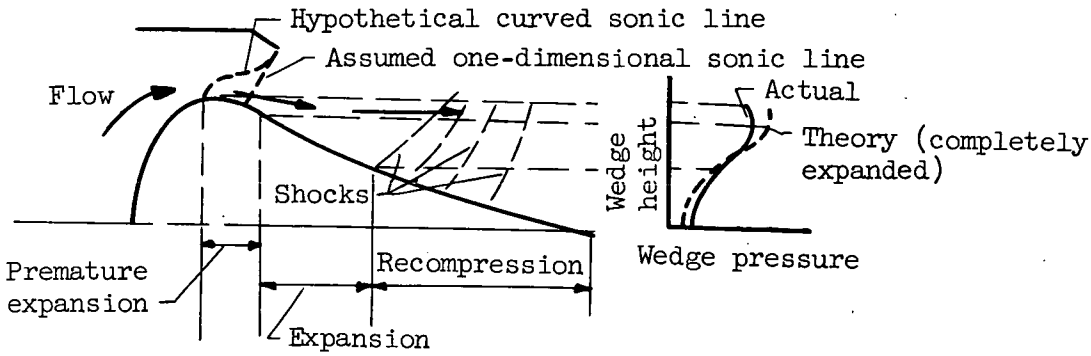

a static pressure somewhat near ambient; then, it recompresses as it turns toward the axial direction. This is illustrated in figure 6, which shows typical wedge-pressure distributions for the wedge nozzle designed for a pressure ratio of 10 operating at overexpanded pressure ratios of 2, 3, 4, and 5. (The theoretical pressure distribution for a nozzle designed for a pressure ratio of 10 is included for comparison.) The losses associated with the expansion-plus-shock recompression process result in the drop in thrust coefficient in the overexpanded region.

As shown in the final sketch, at pressure ratios above the design value (the underexpanded region), nozzle-outlet static pressure and wedge

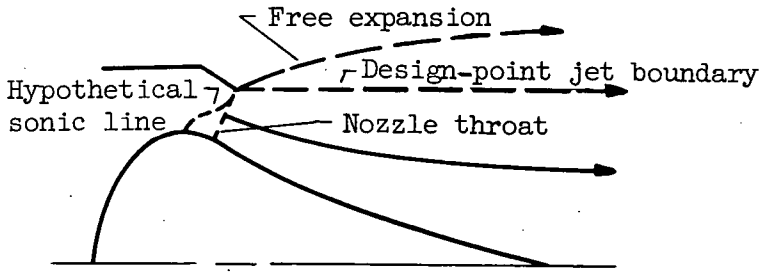

wall pressure stay constant; and the flow continues to expand beyond the confines of the model and the design-point jet boundary. Again the result is a loss of available thrust and, hence, a drop in thrust coefficient.

Another characteristic of the wedge nozzles investigated, which is illustrated in the preceding sketches and by the data in figure 6, is the premature supersonic expansion of the flow around the wedge upstream of the throat as evidenced by low static- to total-pressure ratio. This effect is aggravated by high approach velocities. (A discussion of a

similar effect is given, for instance, in ref. 4 and in ref. 6, p. 835.) A consequence of such premature supersonic flow is a reduction in the nozzle flow capacity (flow coefficient), since at the minimum area the Mach number is not necessarily unity but may vary to values greater or less than unity, and hence the mass flow is less than it would be if the minimum area were filled by sonic flow. A displacement of the sonic line should also distort the entire Prandtl-Meyer expansion field; the evidence of such distortion and its effects will be discussed subsequently along with the specific effects of the geometry variations tested.

Wedge Nozzle Designed for Pressure Ratio of 10

Approach section and side plates. - In figure 7 the performance of the basic wedge nozzle designed for a pressure ratio of 10, configuration 1, is compared with configurations 4, 5, and 6, which have smaller approach sections and reduced side plates. While only a slight variation in thrust with approach-section geometry was noted, the configuration with the smaller approach section showed a marked drop in throat pressure and flow capacity. A comparison of thrust and pressure distributions between these two configurations exemplifies the general observation that departure from the intended flow conditions at the throat (uniform sonic flow) caused by abrupt approach sections need not greatly affect downstream pressure distribution or thrust. With reference to this observation, it might be useful to point out that, whereas supersonic flow upstream of the throat reduces wedge pressures, it also increases the total momentum of the flow at the geometrical throat. Thus the thrust loss due to wedge pressure reduction is partially compensated for, since nozzle thrust may be considered as the sum of the throat axial total momentum and the wedge axial forces (where total momentum is defined as $wV + pA$). A similar observation is also made with regard to the penshape nozzle reported in reference 4.

The 50-percent reduction of the side plates (configurations 4 and 6) reduced the peak thrust coefficient about 1 percent. The concomitant drop in wedge pressure toward the tip and sides of the wedge is shown in figures 7(b) and 8.

Lip angle. - The effect of small changes in lip angle on the performance of the wedge nozzle designed for a pressure ratio of 10 is shown in figure 9. The range of lip angle tested (25.7° to 35.5°) gave only slight thrust-coefficient changes (fig. 9(a)). However, the wedge pressure distributions (fig. 9(b)) show the drop in throat pressure with increasing approach Mach number (decreasing lip angle). The shift of the pressure distribution curves to the left with decreasing lip angle is the result of moving the origin of the Prandtl-Meyer expansion away from the wedge, which allows the higher-pressure regions of the flow fanning out from the lip to intersect the surface farther downstream, as illustrated by the sketches on this figure. The difference in flow capacity

of the nozzles is primarily a result of the difference in the physical throat area.

Wedge Nozzles Designed for Pressure Ratios of 5 and 24

In order to determine possible variations in performance with design pressure ratio, two other Prandtl-Meyer wedge-nozzle configurations with design pressure ratios of 5 and 24 were tested.

Design pressure ratio of 5. - The performance of the wedge nozzle designed for a pressure ratio of 5 is presented in figure 10. Whereas the thrust curve of this configuration shows the expected position of the peak, the wall pressure distributions vary considerably from the theoretical. The fact that the measured pressure on the downstream portion of the wedge is somewhat higher than the theoretical is evidence that the Prandtl-Meyer fan source (the lip exit) was farther down the wedge than intended. In spite of this, however, the performance is as good as could be expected.

Design pressure ratio of 24. - The performance of the wedge nozzle designed for a pressure ratio of 24 is presented in figure 11. As for the previously discussed configurations, the thrust coefficient in the overexpanded region (pressure ratios less than design) is relatively high; thus the thrust curve is relatively flat for the range investigated. Unlike the preceding configurations, however, the corrected airflow curve does not tend to flatten until a pressure ratio of about 9.0 is reached. This effect of pressure ratio on nozzle corrected airflow is felt to be a result of a deflection of the nozzle lip with pressure ratio. Evidence of this is indicated by a comparison of the corrected airflow curve with a curve of lip load factor $(P - p_0)/P$ (where P is constant), which shows that the nozzle corrected airflow increased in the same way as the lip load factor (acting on the cantilevered lip). The resulting change in throat area (as evidenced by the variations in nozzle airflow) would cause a change of equivalent design pressure ratio from about 22 at an operating pressure ratio of 2 to 16 at an operating pressure ratio of 24. (The wall pressure plot (fig. 11(b)) taken at a pressure ratio of 29 corresponds well to the theoretical curve for a wedge designed for a pressure ratio of 20.) These data are still considered representative of high-pressure-ratio wedges, however, since the change in throat area increased the equivalent design pressure ratio at low operating pressure ratios, thus exaggerating any possible performance loss due to overexpansion.

Shortened Wedge Nozzle

Any reduction in nozzle size without thrust penalty is desirable; such an attempt was made with configurations 9, 10, and 11 (design-

pressure ratio about 9, fig. 2), which were approximately two-thirds as long as the corresponding Prandtl-Meyer wedge-nozzle design.

Experience with plug nozzles (ref. 3) showed that method-of-characteristics (curve surface) plugs performed better than did conical plugs, not only at design pressure ratio but also below design, where the characteristics plugs were no longer correctly shaped for isentropic expansion. A curved instead of a straight wedge profile was therefore selected as a more promising nonisentropic (shortened) wedge nozzle.

The performance of the shortened wedge is presented in figure 12. The maximum thrust coefficients were about 2 percentage points lower than those of the Prandtl-Meyer designs. The most abbreviated lip (configuration 9) showed poorest thrust and pressure distributions. Lengthening the lip and reducing the wedge hump (configuration 10) allowed lower approach Mach number and, consequently, closer approach to the ideal straight sonic line at the throat. Thrust and pressure distributions of this configuration evidenced closer approximation to isentropic expansion with some improvement in thrust at lower pressure ratios. (A theoretical pressure distribution for a wedge nozzle having the same maximum thrust pressure ratio as configuration 11 is included in fig. 12 for comparison.) A reduction in shroud dimension (configuration 11) increased the approach Mach number and the throat overexpansion. Peak thrust was little changed but was shifted to a higher pressure ratio as a result of the decreased throat- to exit-area ratio of this configuration (fig. 4).

Comparison of Prandtl-Meyer Wedge Nozzles with Other Nozzles

In figure 13 the thrust curves of the Prandtl-Meyer wedge nozzles are compared with those of the best plug and convergent-divergent nozzles previously tested at the NACA Lewis laboratory (refs. 1 and 3). The peak wedge-nozzle thrust is shown as about 1 percent lower than that of the plug and convergent-divergent nozzles. At pressure ratios considerably below design, the wedge nozzles show thrust coefficients considerably better than those of the convergent-divergent nozzle but not as good as those of the plug nozzle. In no case is the thrust coefficient more than $3\frac{1}{2}$ percentage points below the design value at pressure ratios less than design. The superiority of the wedge nozzle designed for a pressure ratio of 5 over the convergent nozzle is evident, indicating its possible use in turbojet aircraft in the Mach number range of 1 to 2.

Application to Aircraft

Throat-area variation. - The tests of lip-angle effect showed little change in thrust with a mass-flow variation of 20 percent (fig. 9). An estimate of the effects of wider mass-flow variations may be made from the thrust curve of the wedge nozzle designed for a pressure ratio of 24. As shown in the following sketch, this nozzle may be considered as an approximation of a wedge nozzle designed for a pressure ratio of 10 with lip angle increased to restrict the mass flow to 42 percent of the design value of the latter nozzle:

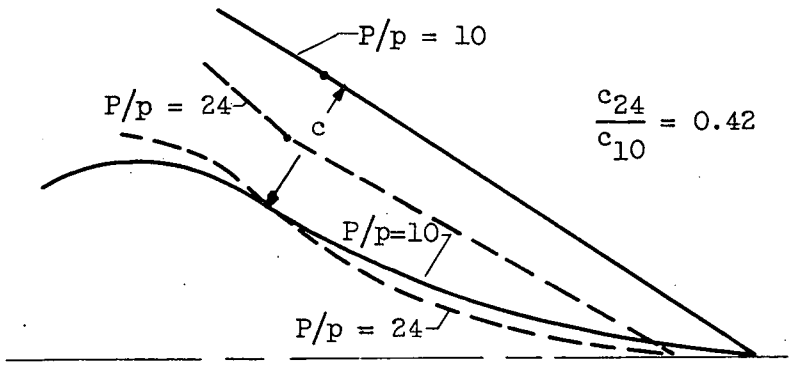

The thrust of these two wedges is almost the same for all operating pressure ratios below 10 (fig. 13). From this it is inferred that throat-area decreases may be made with little change in low-pressure-ratio internal performance by simply increasing the lip angle.

Increases in throat area (and approach Mach number), on the other hand, tend to cause premature supersonic flow and excessive overexpansion in the lip region. While the data of this report do not show excessive thrust losses from such overexpansion, plug data (ref. 3) from more extensively varied configurations do show effects which, in most cases, are small. For maximum internal performance, then, it seems advisable to vary the throat area to smaller-than-design values rather than in the other direction whenever possible. It must be remembered, however, that high lip angles contribute to high external drag.

External conformation. - The rectangular-throat wedge nozzle may not conform well in many installations which have rounded forebodies. The throat of this wedge nozzle can be modified to other throat shapes by tracing the Prandtl-Meyer streamlines from the desired throat boundaries. (This method is illustrated in ref. 7 and was applied to the penshape nozzle of ref. 4.) The resultant configuration would conform well with traditional afterbody shapes and would be compatible with iris

or clamshell lips (for throat-area variations). Installed, this wedge nozzle would look as shown in the following sketch:

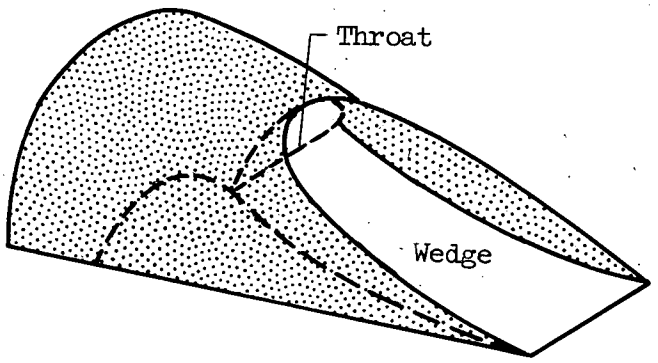

External-flow effects. - The wedge nozzle, like any other nozzle, will be affected by the external pressure field adjacent to it. Low pressures around the jet exit will effectively increase the nozzle pressure ratio, causing the nozzle flow to expand more than it would otherwise, thereby reducing wedge pressure and, hence, thrust. For an extreme afterbody design, wedge or plug nozzles could show the same overexpansion losses as does the convergent-divergent nozzle, whose shielded jet cannot be affected by external pressure over a wide range of low-pressure-ratio operation.

Additional information is required to optimize the external and internal configuration, since internal performance is enhanced by lip angles close to the theoretical values while external drag, including the low-pressure-field effect on internal performance, is minimized by low lip angles. (Some effects of lip angle and boattail design on plug-nozzle performance are given in ref. 8, in which it is shown that conical boattails greatly reduce the lip drag and internal overexpansion over those obtained with cylindrical boattails.)

Thus the wedge nozzle appears to be competitive with other types in internal performance; and its use seems worthy of consideration in cases where it provides secondary advantages in base drag reduction, ease of cooling, or the like.

CONCLUDING REMARKS

The three Prandtl-Meyer wedge nozzles tested (design pressure ratios of 5, 10, and 24) showed peak thrust coefficients about 1 percent lower than those of the best convergent-divergent and plug nozzles investigated to date. Thrust at all pressure ratios below design was within $3\frac{1}{2}$ percentage points of peak thrust.

Variations in approach-section size and lip angle had negligible effect on thrust over the ranges tested, and a 50-percent reduction in side-plate coverage caused about a 1-percentage-point thrust loss.

A wedge designed for a pressure ratio of about 9 with 30-percent reduction in length from the Prandtl-Meyer design showed peak thrust coefficients about 2 percent below those of the best Prandtl-Meyer designs tested.

The wedge nozzle appears to be competitive with other types on the basis of internal performance. Its use seems worthy of consideration in cases where it provides secondary advantages in base drag reduction, ease of cooling, or the like.

Lewis Flight Propulsion Laboratory
National Advisory Committee for Aeronautics
Cleveland, Ohio, December 4, 1956

APPENDIX A

SYMBOLS

A	area, sq in.
A_e	throat area measured normal to lip at exit, sq in.
A_l	pipe area under labyrinth seal, sq in.
C_F	jet-thrust coefficient
C_w	flow coefficient
c	throat depth
F	jet thrust, lb
F_d	balanced-air-pressure diaphragm reading, lb
g	acceleration due to gravity, 32.17 ft/sec^2
h	wedge-nozzle height
P	total pressure, lb/sq in.
p	static pressure, lb/sq in.
p_{bm}	integrated static pressure acting on outside of bellmouth, lb/sq in.
R	gas constant, 53.35 ft-lb/(lb)(^oR)
T	total temperature, ^oR
V	velocity, ft/sec
w	mass flow, slugs/sec
w_a	airflow, lb/sec
β	lip angle, deg
γ	ratio of specific heats
δ	ratio of nozzle-inlet total pressure to NACA standard sea-level pressure of 2116 lb/sq ft

θ ratio of nozzle-inlet total temperature to NACA standard sea-level temperature of 518.7° R

Subscripts:

d design

e exit

eff effective

id ideal

m measured

w wedge wall

0 ambient, exhaust-nozzle outlet

1 bellmouth inlet

2 air measuring station

3 exhaust-nozzle inlet

APPENDIX B

METHODS OF CALCULATION

Airflow was calculated as the summation of the flow across station 2 (fig. 4):

$$w_a = \sum_{A_2} \left(\frac{w\sqrt{gRT}}{pA} \right) \frac{\Delta A \, p_2 g}{\sqrt{gRT_2}}$$

where

$$\frac{w\sqrt{gRT}}{pA} = \left(\frac{p}{P} \right)^{\frac{1-\gamma}{\gamma}} \sqrt{\frac{2\gamma}{\gamma - 1} \left(1 - \frac{p}{P} \right)^{\frac{\gamma-1}{\gamma}}}$$

is the local value found from each of the eight total-pressure probes and the wall static-pressure taps at station 2. The term ΔA is the area sampled by the individual probes.

Jet thrust was defined as

$$F = wV_{e,eff} + A_e(p_{e,eff} - p_0)$$

The measured jet thrust was found as

$$F_m = w_m V_1 + p_1 A_1 - p_{bm} A_1 + a_1(p_{bm} - p_0) - F_d$$

The ideally available jet thrust, based on measured mass flow, was calculated as

$$F_{id} = w_m \sqrt{\frac{2R}{g} \frac{\gamma}{\gamma - 1} T_3 \left[1 - \left(\frac{p_0}{P_3} \right)^{\frac{\gamma-1}{\gamma}} \right]}$$

Thrust coefficient, the ratio of measured to ideal thrust, was

$$C_F = F_m / F_{id}$$

REFERENCES

1. Krull, H. George, and Beale, William T.: Internal Performance Characteristics of Short Convergent-Divergent Exhaust Nozzles Designed by the Method of Characteristics. NACA RM E56D27a, 1956.

2. Greathouse, William K., and Beale, William T.: Performance Characteristics of Several Divergent-Shroud Aircraft Ejectors. NACA RM E55G21a, 1955.

3. Krull, H. George, Beale, William T., and Schmiedlin, Ralph F.: Effect of Several Design Variables on Internal Performance of Convergent-Plug Exhaust Nozzles. NACA RM E56G20, 1956.

4. Connors, James F., and Meyer, Rudolph C.: Investigation of an Asymmetric "Penshape" Exit Having Circular Projections and Discharging into Quiescent Air. NACA RM E56K09a, 1957.

5. Connors, J. F., and Meyer, Rudolph C.: Design Criteria for Axisymmetric and Two-Dimensional Supersonic Inlets and Exits. NACA TN 3589, 1956.

6. Shapiro, Ascher H.: The Dynamics and Thermodynamics of Compressible Fluid Flow. Vol. II. The Ronald Press Co., 1954.

7. Evvard, John C., and Maslen, Stephen H.: Three-Dimensional Supersonic Nozzles and Inlets of Arbitrary Exit Cross Section. NACA TN 2688, 1952.

8. Salmi, R. J., and Cortright, E. M., Jr.: Effects of External Stream Flow and Afterbody Variations on the Performance of a Plug Nozzle at High Subsonic Speeds. NACA RM E56F11a, 1956.

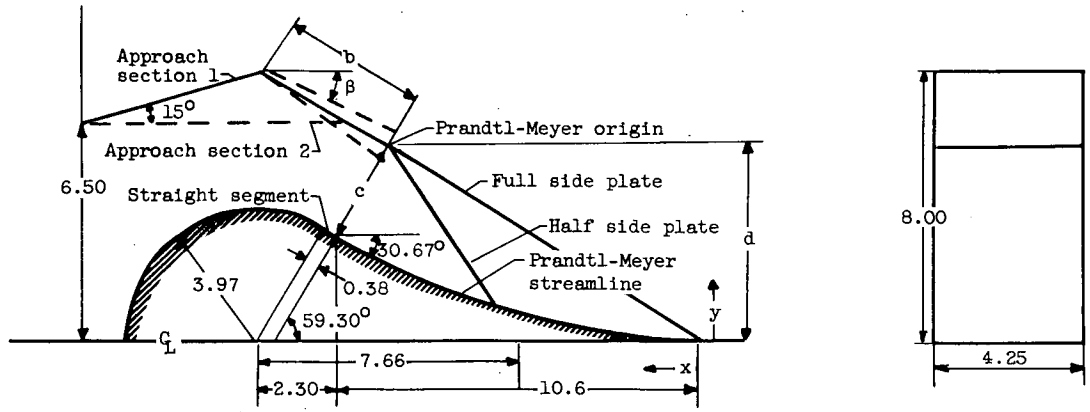

x	10.698	9.847	9.446	9.089	9.202	8.418	8.076	7.724	7.358	6.969	6.567	6.118	5.681	5.202	4.673	4.139	3.550	2.926	2.260	1.561	0.808	0
y	3.220	2.715	2.490	2.290	2.113	1.950	1.781	1.540	1.483	1.334	1.189	1.050	0.919	0.786	0.658	0.539	0.433	0.330	0.238	0.160	0.097	0.048

Configuration	Description	b	c	d	β, deg	Approach section	Side plate
1	Large approach section, basic isentropic design	4	3.02	5.8	30.67	1	Full
2	Decreased throat area	4	2.72	5.55	35.5	1	Full
3	Increased throat area	4	3.33	6.15	25.7	1	Full
4	Reduced-side-plate coverage	4	3.02	5.8	30.67	1	Half
5	Reduced approach section	1.23	3.05	5.8	30.67	2	Full
6	Reduced approach section, reduced side plate	1.23	3.05	5.8	30.67	2	Half

(a) Configurations 1 to 6; design pressure ratio, 10.

Figure 1. - Prandtl-Meyer wedge nozzles. (Dimensions are in inches.)

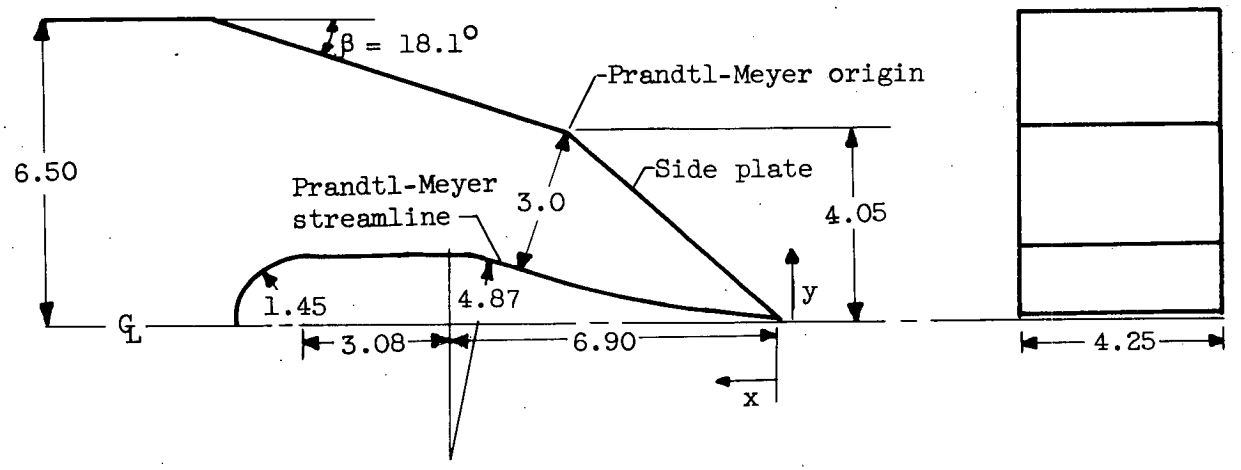

x	5.391	4.451	4.001	3.618	3.250	2.890	2.519	2.142	1.753	1.341	0.917	0.467	0
y	1.249	0.942	0.806	0.691	0.592	0.506	0.416	0.346	0.282	0.220	0.176	0.124	0.095

(b) Configuration 7; design pressure ratio, 5.

Figure 1. - Continued. Prandtl-Meyer wedge nozzles. (Dimensions are in inches.)

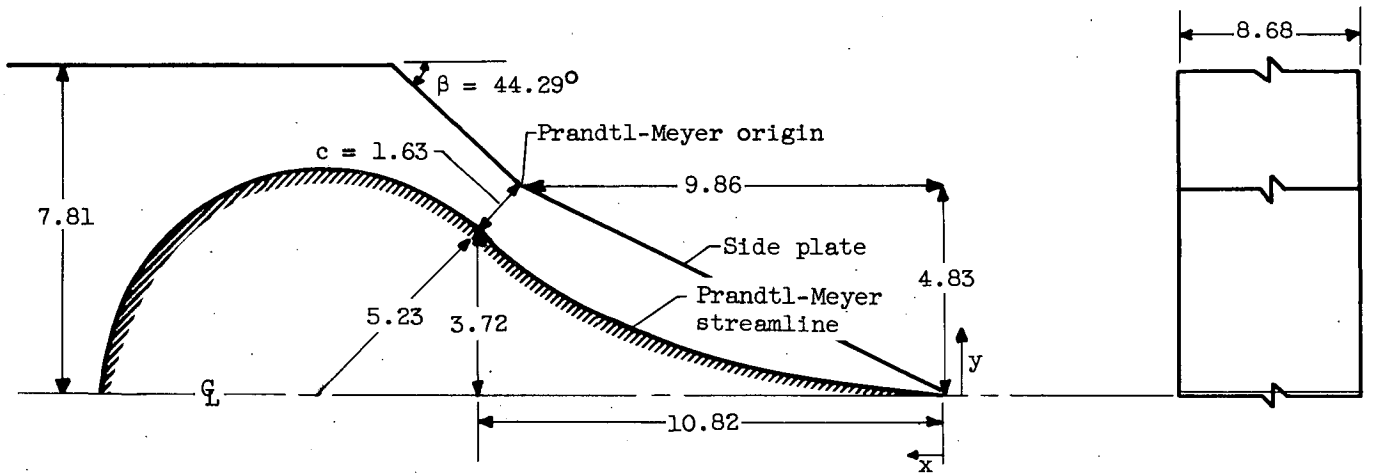

x	10.846	10.504	10.340	10.201	10.060	9.922	9.708	9.632	9.479	9.315	9.141	8.956	8.757	8.546	8.315	8.075	7.811
y	3.735	3.401	3.246	3.117	2.991	2.875	2.760	2.647	2.534	2.420	2.307	2.192	2.075	1.958	1.837	1.722	1.602

x	7.531	7.231	6.908	6.562	6.192	5.794	5.369	4.917	4.435	3.909	3.357	2.763	2.136	1.465	0.7516	0
y	1.482	1.364	1.250	1.127	1.012	0.896	0.785	0.677	0.575	0.472	0.452	0.292	0.216	0.144	0.084	0.060

(c) Configuration 8; design pressure ratio, 24.

Figure 1. - Concluded. Prandtl-Meyer wedge nozzles. (Dimensions are in inches.)

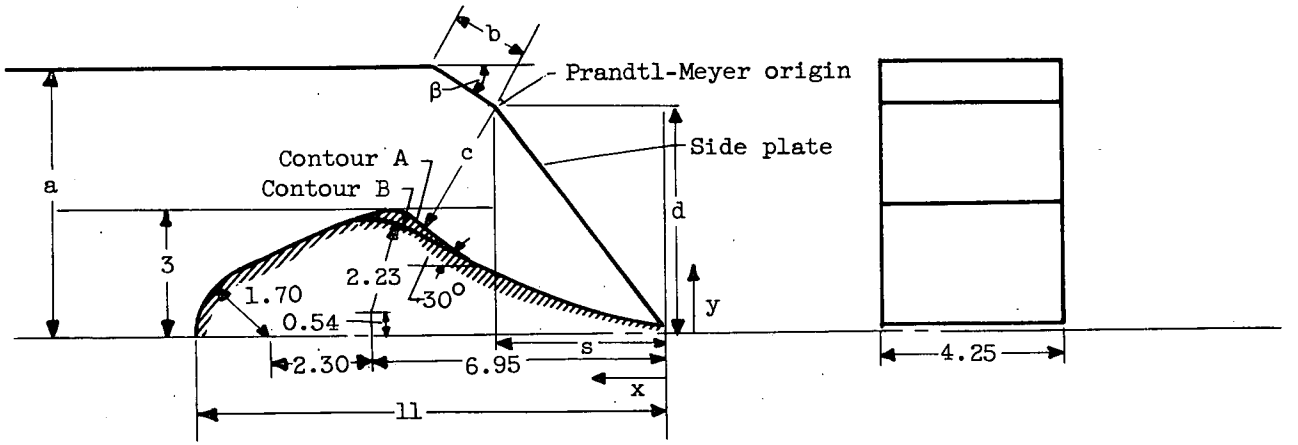

Contour A

x	0	0.40	0.85	1.21	1.61	2.01	2.41	2.82	3.22	3.62	4.02	4.42	4.83	5.23	5.63	5.84	5.96	6.20	6.43
y	0.145	0.202	0.282	0.379	0.483	0.596	0.730	0.877	1.05	1.23	1.44	1.67	1.82	2.20	2.53	2.70	2.79	2.94	3.00

Configuration	Description	a	b	c	d	s	β, deg	Wedge contour	Geometrical area ratio, d/c	Equivalent design pressure ratio
9	Short lip	6.45	1.00	3.40	5.92	4.69	33.0	A	1.74	8.2
10	Long lip	6.45	3.85	2.46	4.38	4.40	33.0	B	1.78	8.6
11	Reduced frontal area	5.20	1.30	2.47	4.65	4.90	30.0	B	1.88	9.6

Figure 2. - Shortened wedge nozzle. (Dimensions are in inches.)

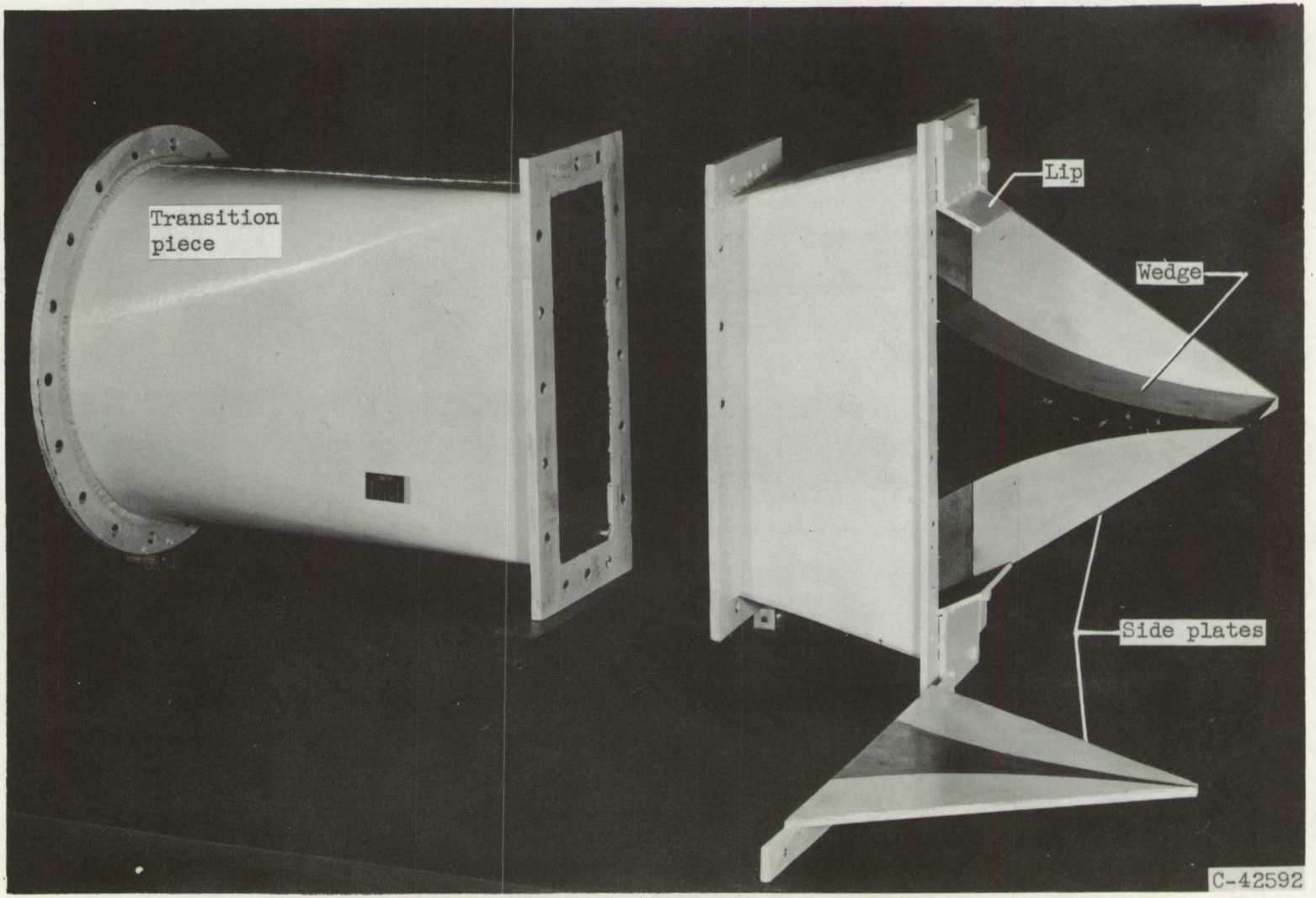

Figure 3. - Typical wedge nozzle. Configuration 1.

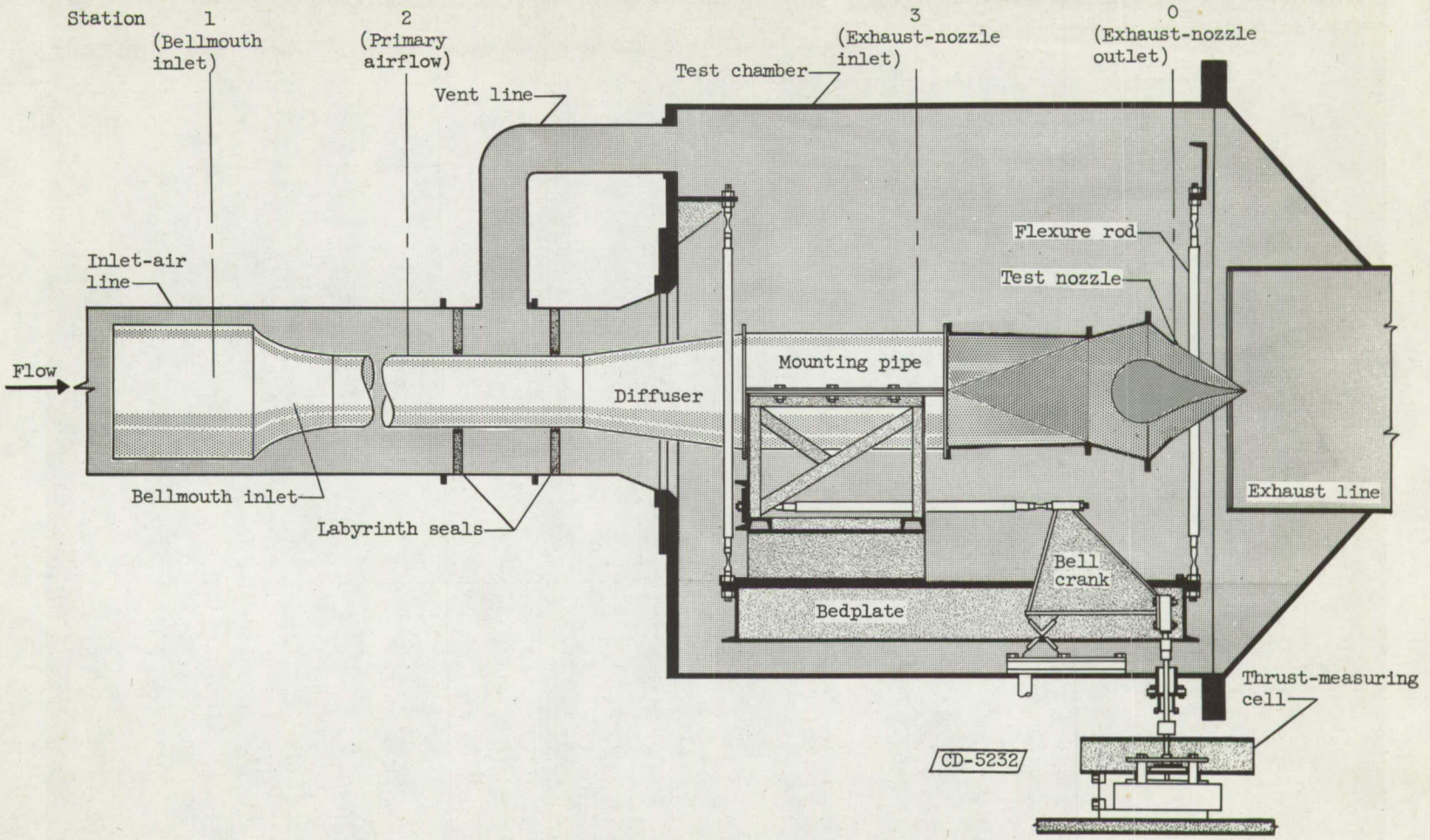

Figure 4. - Schematic drawing of test facility.

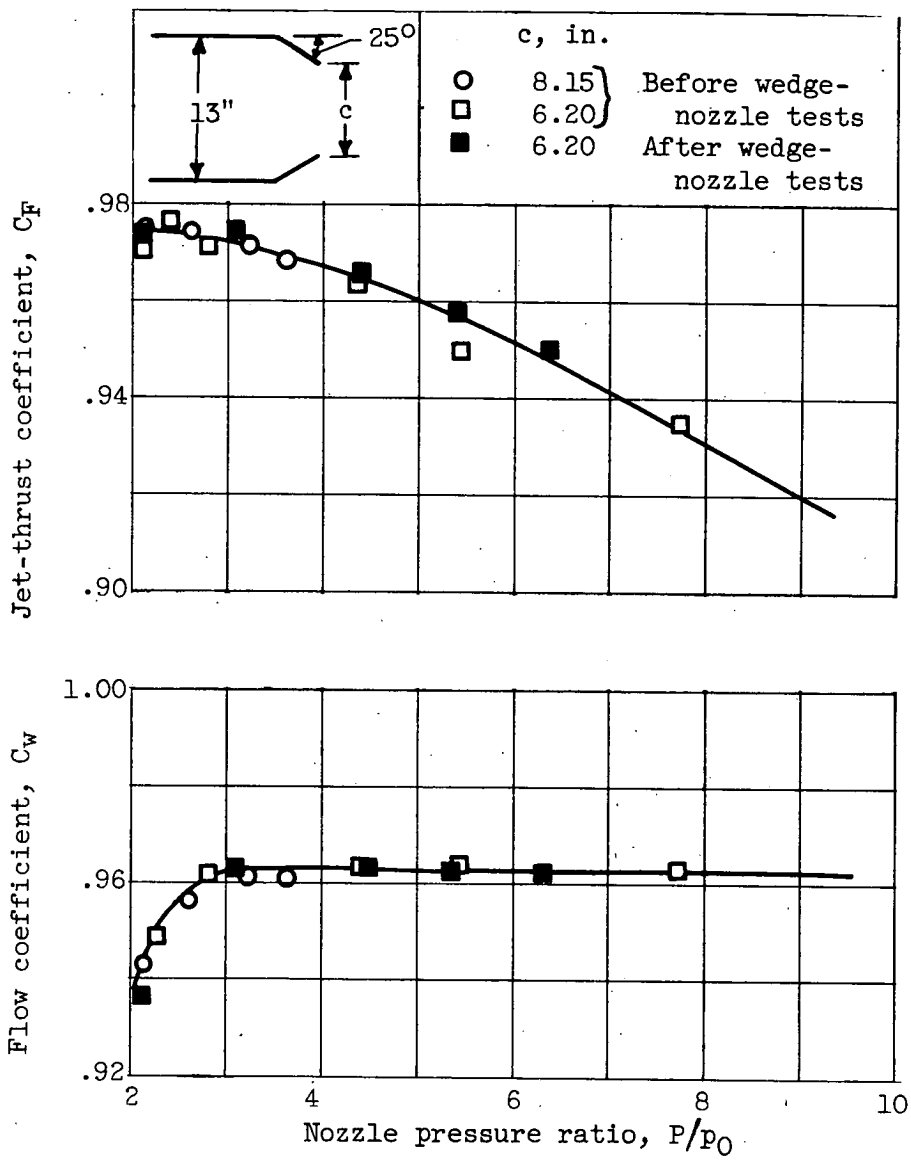

Figure 5. - Repeatability tests of convergent nozzles.

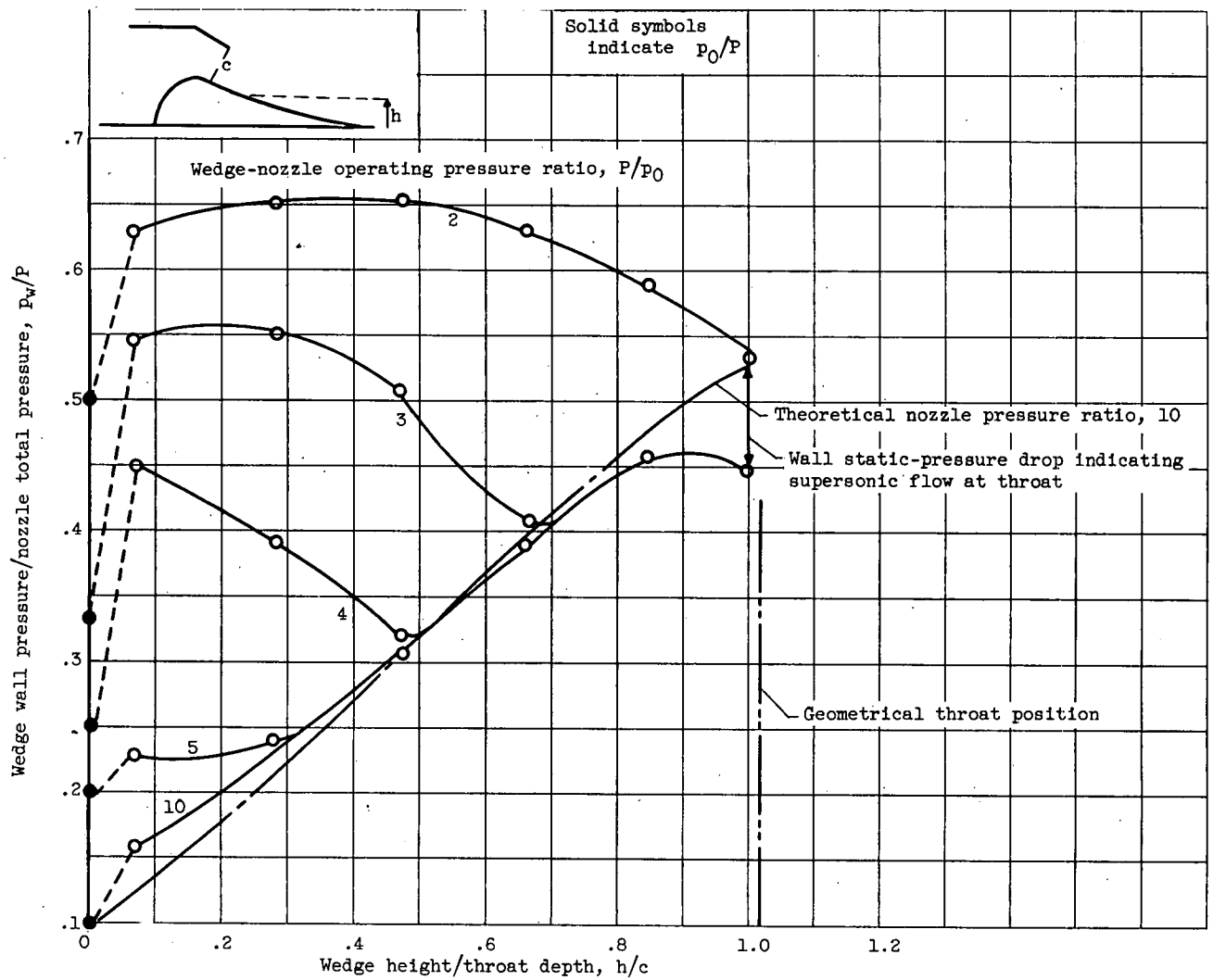

Figure 6. - Typical off-design wedge surface pressure distributions of Prandtl-Meyer wedge nozzle. Design pressure ratio, 10; configuration 1.

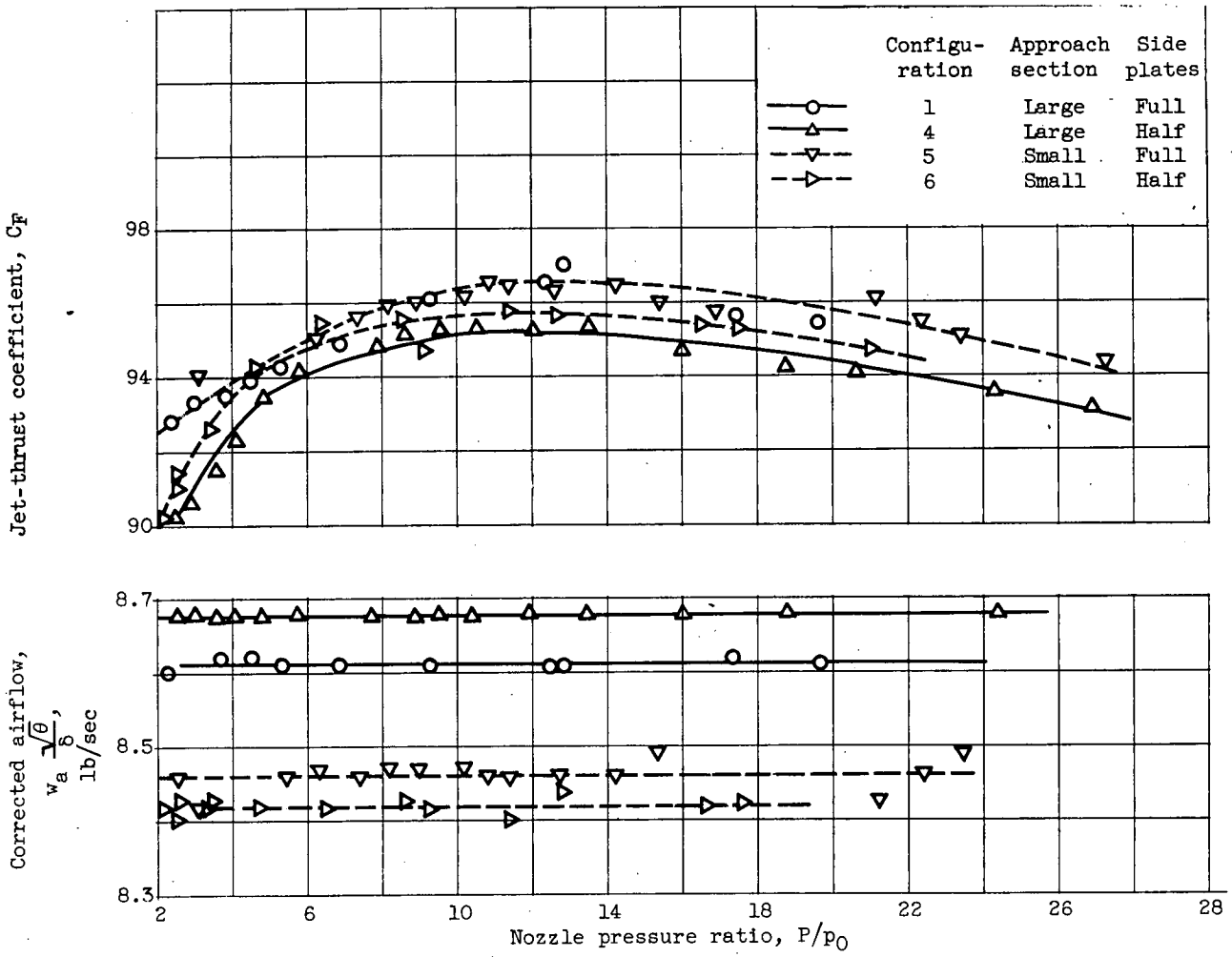

(a) Thrust and flow characteristics.

Figure 7. - Effect of approach geometry and side-plate coverage on performance of Prandtl-Meyer wedge nozzle. Design pressure ratio, 10.

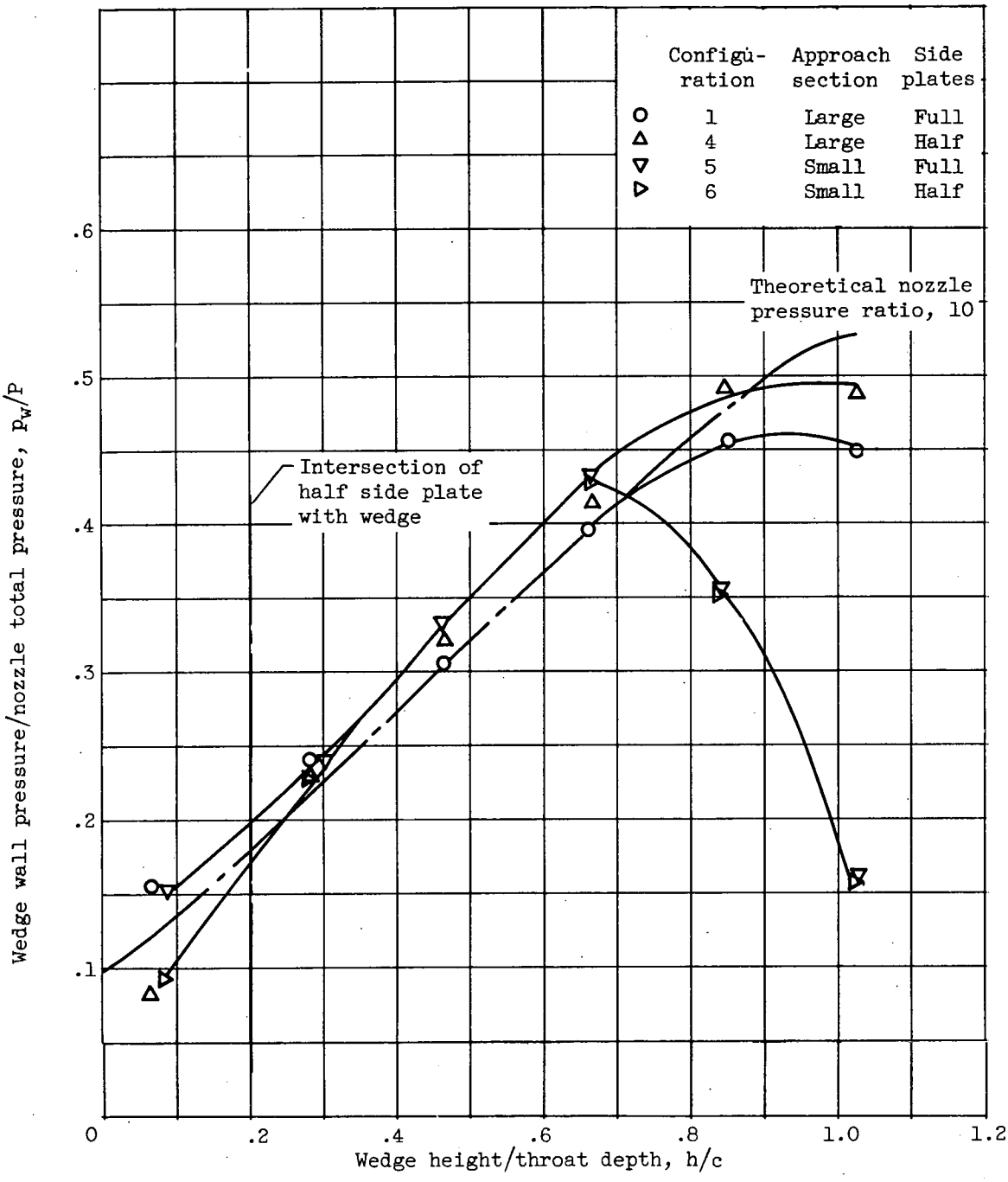

(b) Wedge surface pressure distributions; operating pressure ratio, 15.

Figure 7. - Concluded. Effect of approach geometry and side-plate coverage on performance of Prandtl-Meyer wedge nozzle. Design pressure ratio, 10.

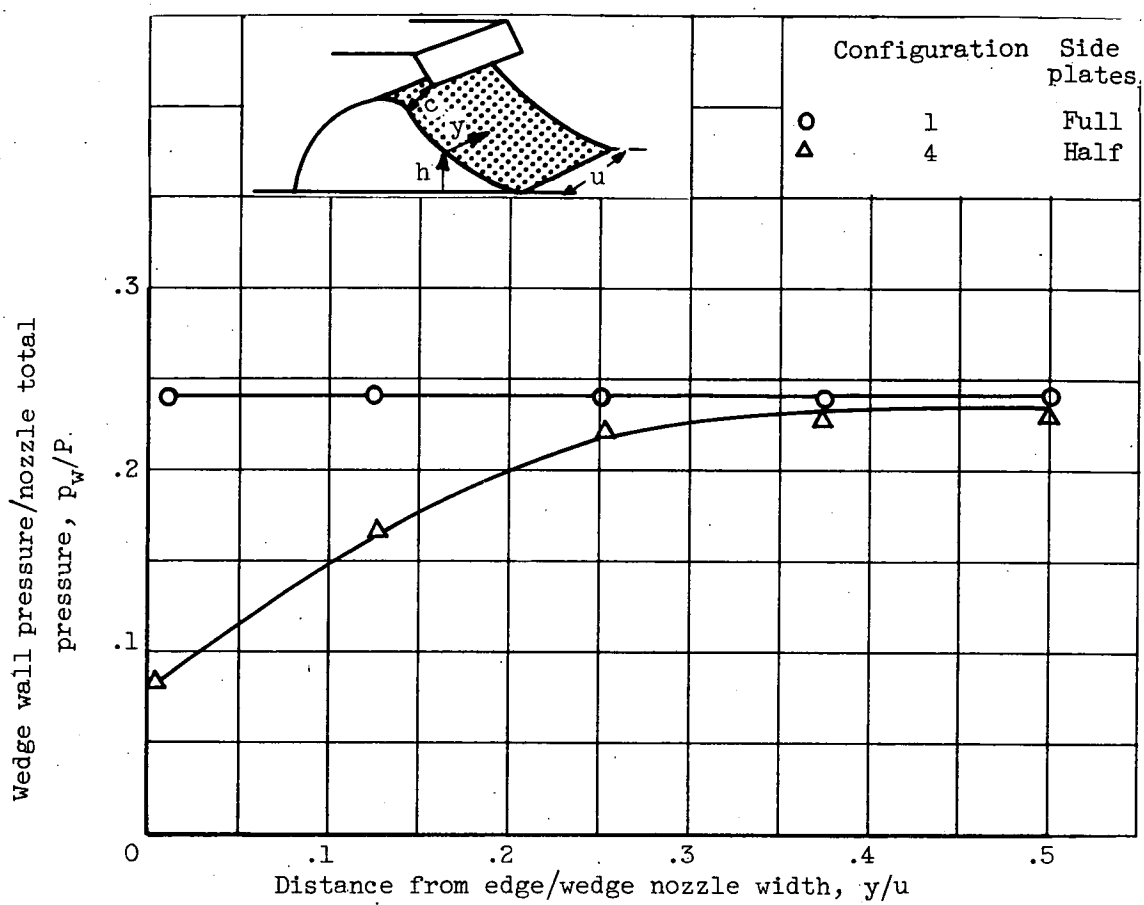

Figure 8. - Effect of side-plate coverage on transverse wedge surface pressures. Operating pressure ratio, 15; large approach section; h/c, 0.28.

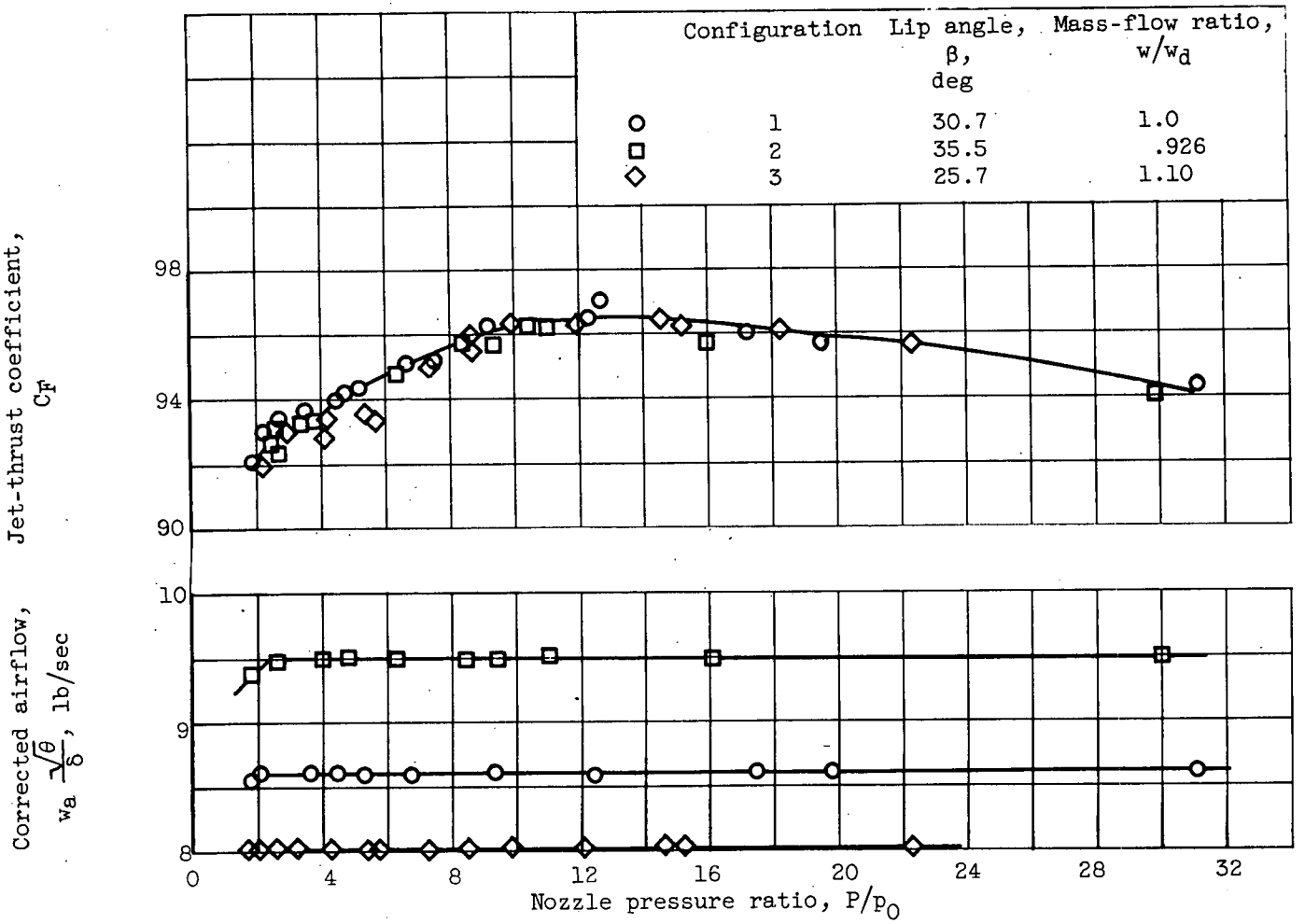

(a) Thrust and flow characteristics.

Figure 9. - Effect of small changes in lip angle on performance of Prandtl-Meyer wedge nozzle. Design pressure ratio, 10.

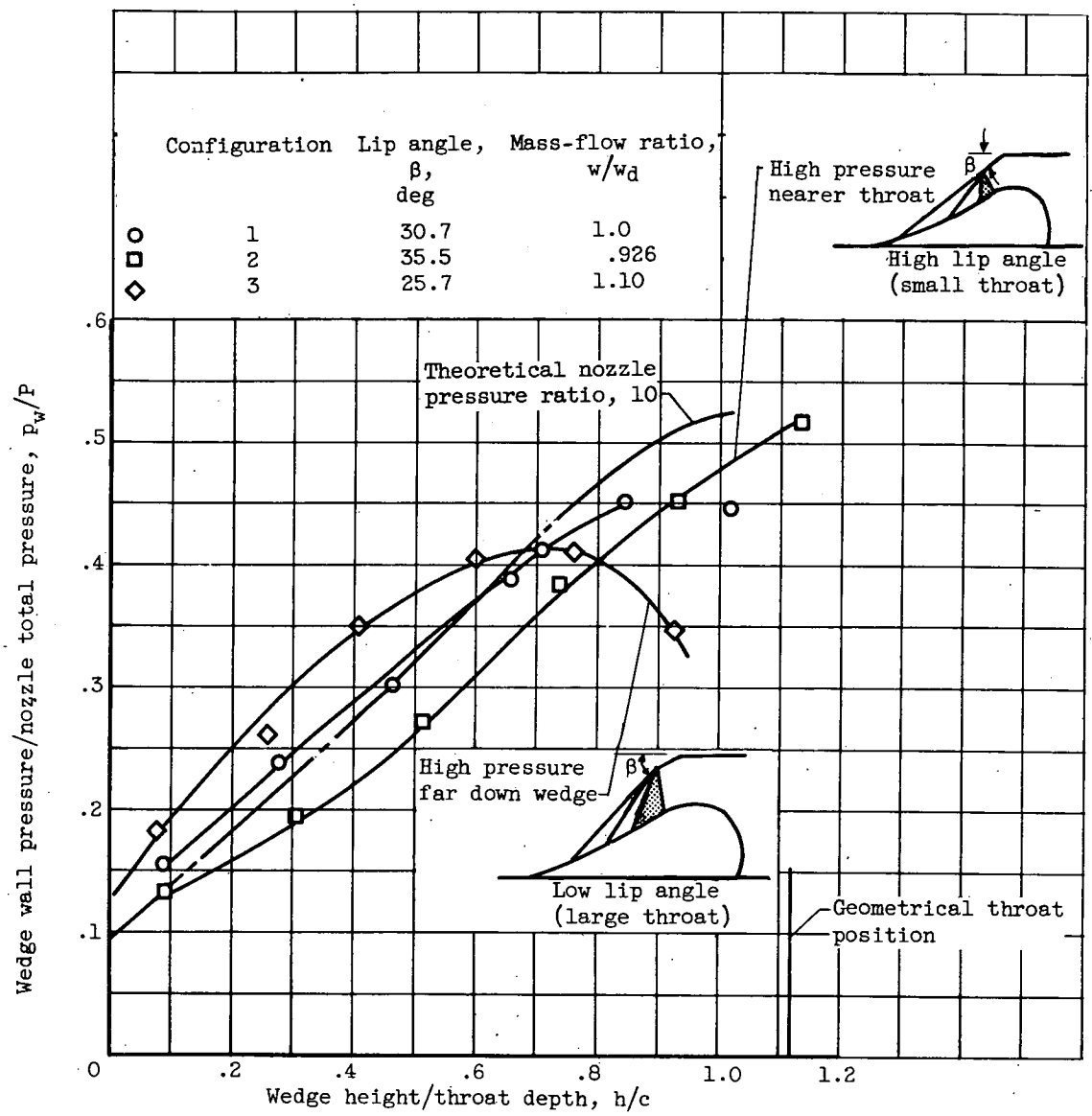

(b) Wedge surface pressure distributions; operating pressure ratio, 15.

Figure 9. - Concluded. Effect of small changes in lip angle on performance of Prandtl-Meyer wedge nozzle. Design pressure ratio, 10.

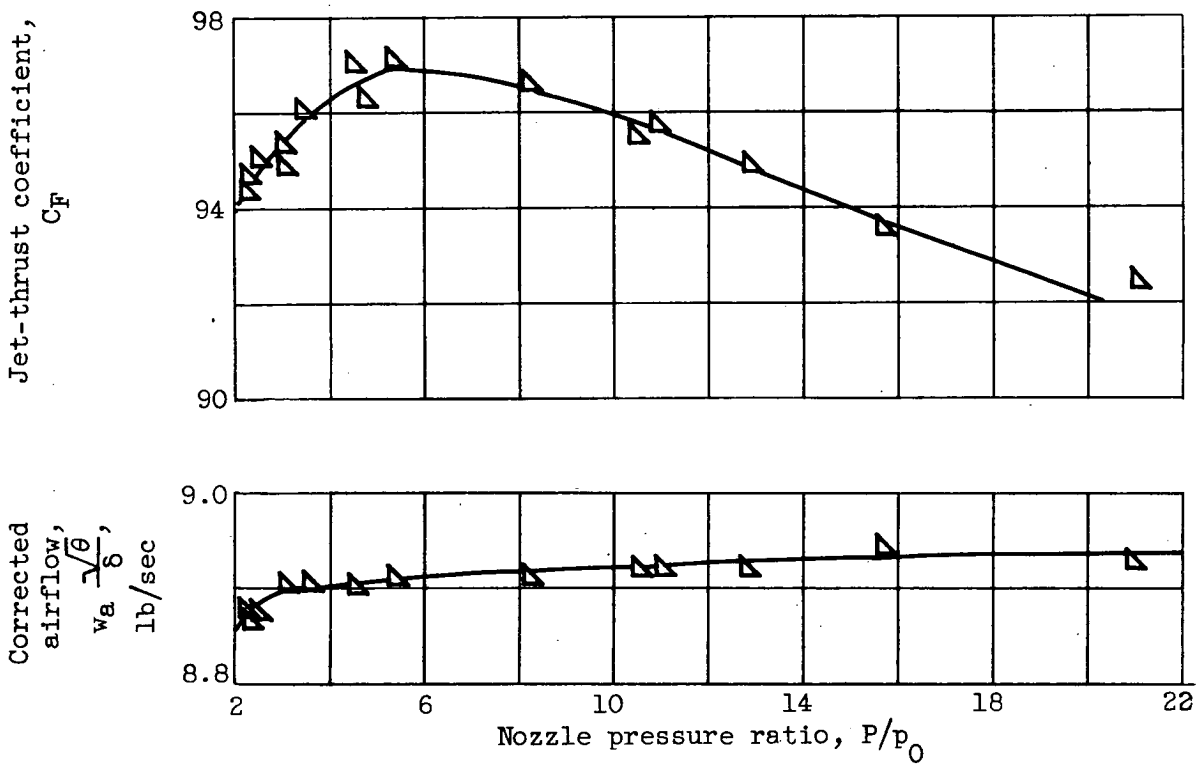

(a) Thrust and flow characteristics.

Figure 10. - Performance of Prandtl-Meyer wedge nozzle designed for pressure ratio of 5. Configuration 7.

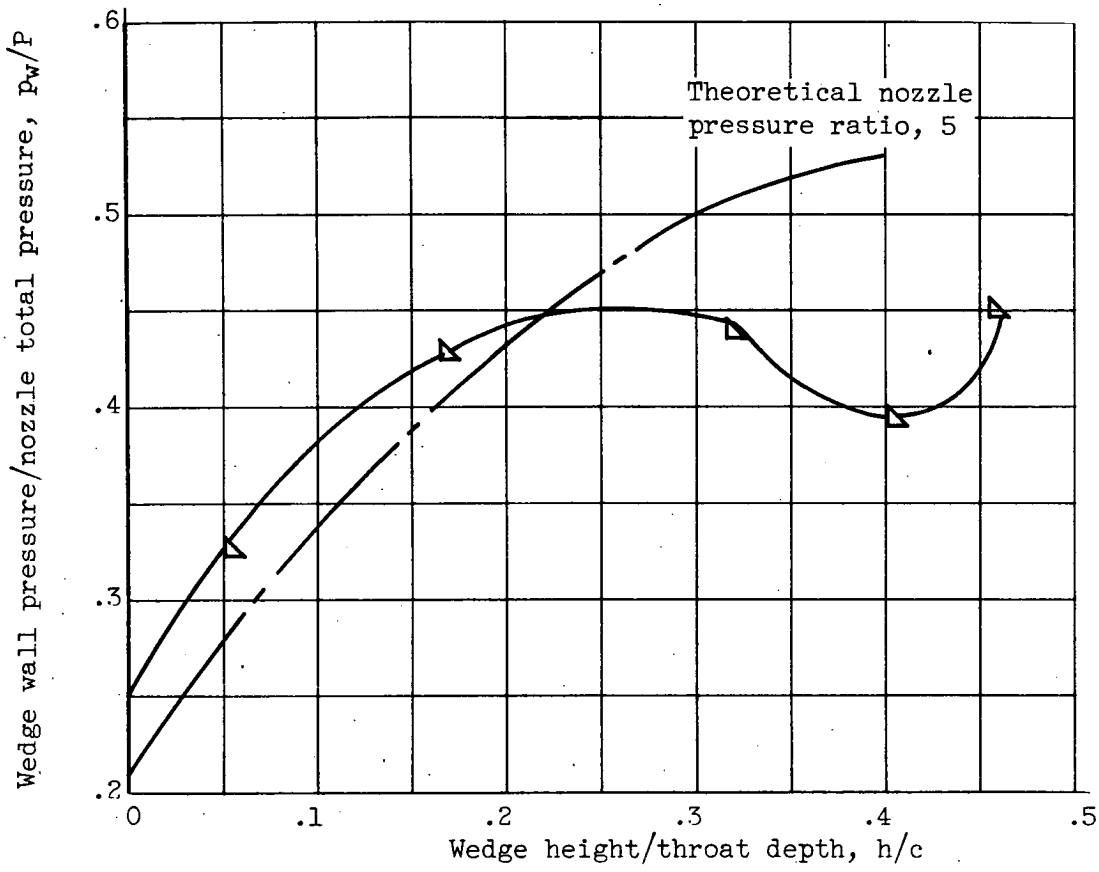

(b) Wedge surface pressure distribution; operating pressure ratio, 10.

Figure 10. - Concluded. Performance of Prandtl-Meyer wedge nozzle designed for pressure ratio of 5. Configuration 7.

(a) Thrust and flow characteristics.

Figure 11. - Performance of Prandtl-Meyer wedge nozzle designed for pressure ratio of 24. Configuration 8.

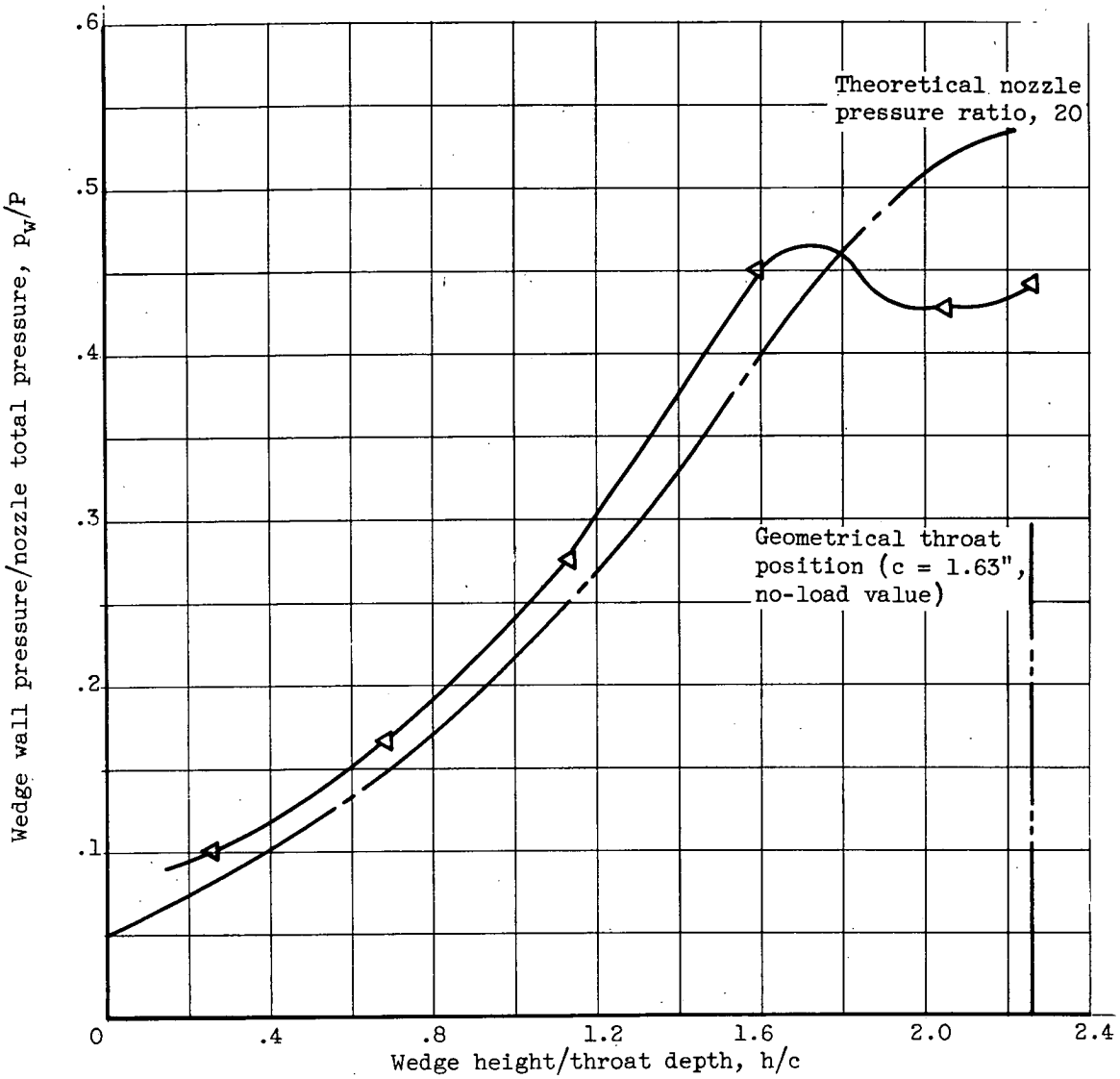

(b) Wedge surface pressure distribution; operating pressure ratio, 29.

Figure 11. - Concluded. Performance of Prandtl-Meyer wedge nozzle designed for pressure ratio of 24. Configuration 8.

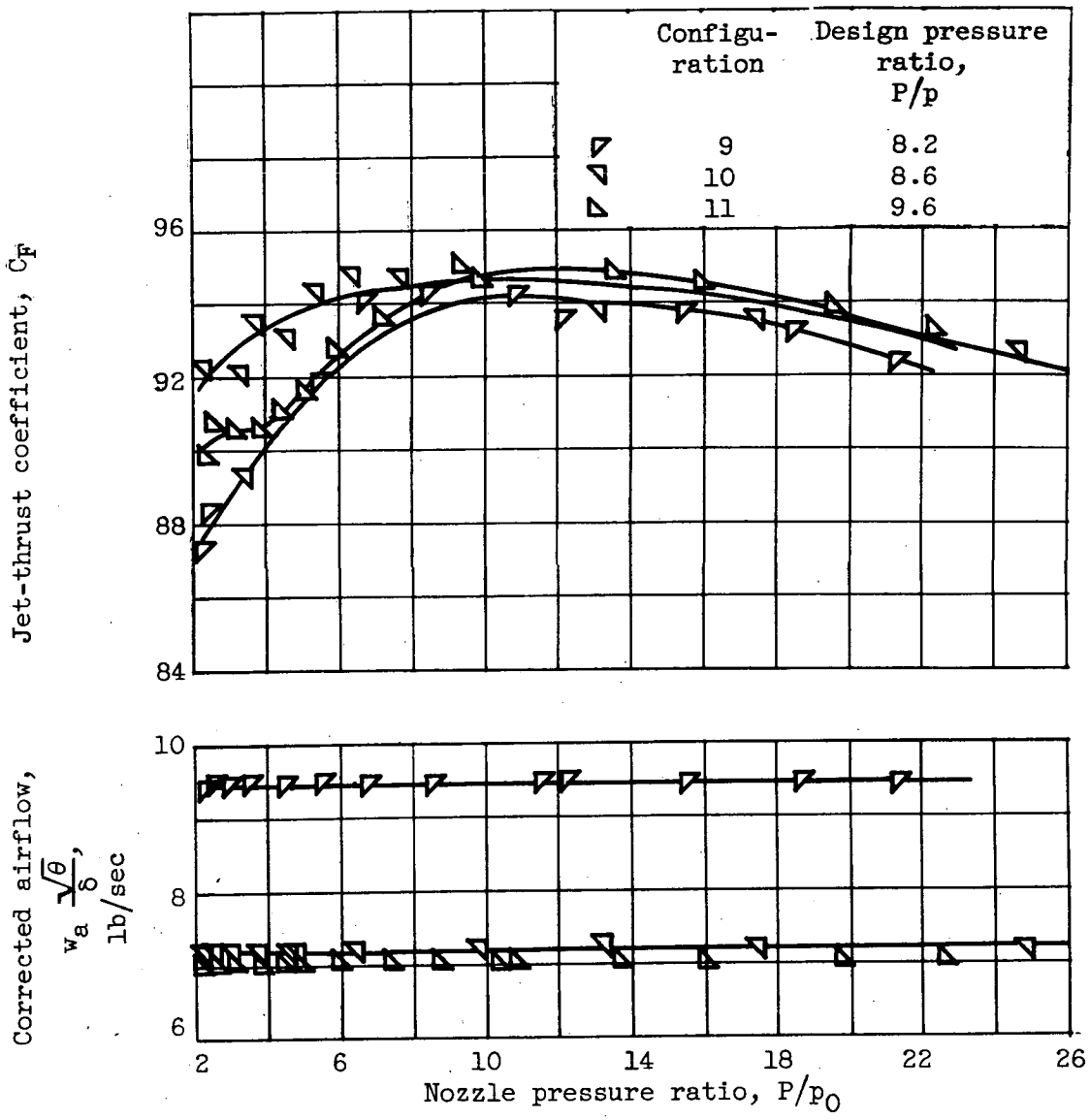

(a) Thrust and flow characteristics.

Figure 12. - Performance of shortened wedge nozzle.

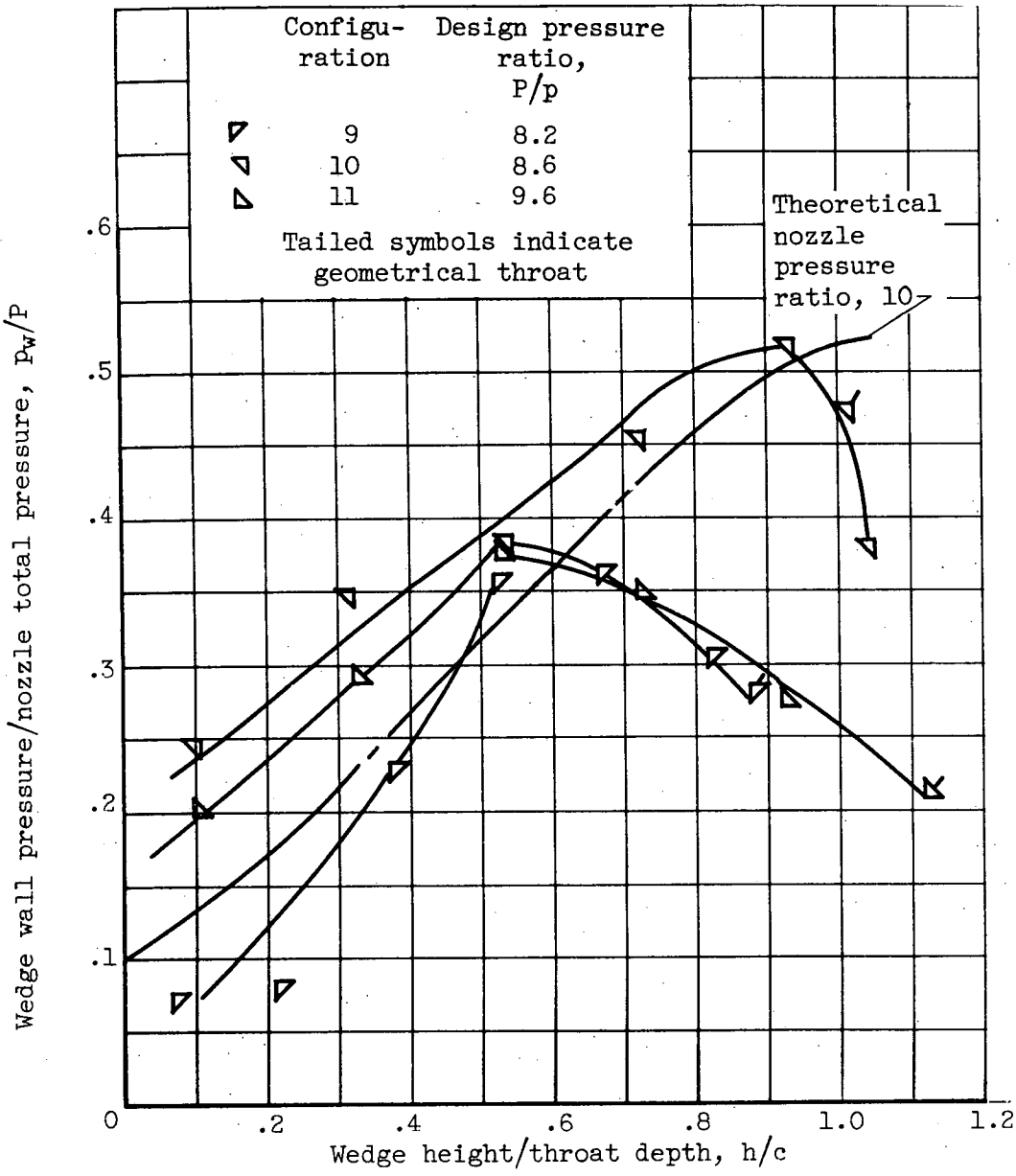

(b) Wedge surface pressure distributions.

Figure 12. - Concluded. Performance of shortened wedge nozzle.

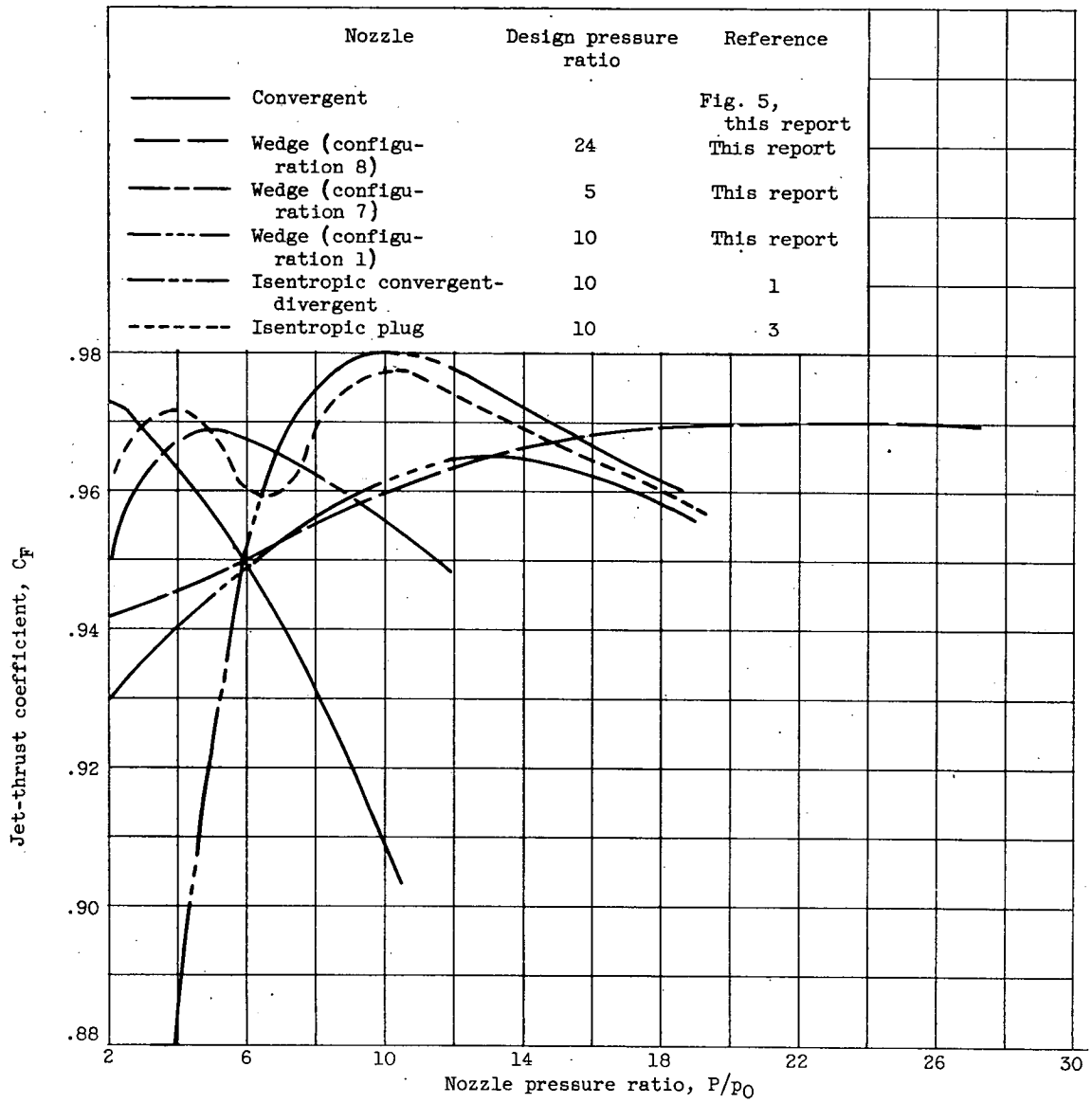

Figure 13. - Comparison of Prandtl-Meyer wedge nozzles with other nozzles.